DALTON
FULL PAPER

# Octahedral tilting and ordering of vacancies in the fast ion conductor $Li_{0.12}La_{0.63}TiO_3$ perovskite: a neutron diffraction study

**J. Sanz,*[a] J. A. Alonso,[a] A. Varez[b] and M. T. Fernández-Díaz[c]**

[a] *Instituto de Ciencia de Materiales, CSIC, Cantoblanco, E-28049, Madrid, Spain. E-mail: jsanz@icmm.csic.es*
[b] *Dpto. Materiales, Universidad Carlos III de Madrid, E-28911, Leganés, Spain*
[c] *Institut Laue-Langevin, F-38045, Grenoble, France*

***Received 30th October 2001, Accepted 14th January 2002***
***First published as an Advance Article on the web 5th March 2002***

We have examined by neutron powder diffraction (NPD) a Li-poor member of the $Li_{3x}La_{\frac{1}{3}-x}TiO_3$ series, with $x = 0.04$, which exhibits one of the highest reported values of ionic conductivity. The unit cell deduced, a $2a_o \times 2a_o \times 2a_o$ superstructure of the elementary perovskite unit ($a_o \approx 3.8$ Å), results from two superimposed effects: the out-of-phase tilting of the $TiO_6$ octahedra along the *b* crystallographic axis, and the ordering of La vacancies, preferentially occupying the $z/c = 0.5$ over the $z/c = 0$ layers. In this superstructure, defined in the *Cm*2*m* space group, a bi-dimensional conductivity is favored by the alternating disposition of lanthanum and cation vacancies in consecutive planes along the *c*-axis. A difference Fourier synthesis suggests that Li cations are located close to the square windows defined by four $TiO_6$ octahedra, as previously shown in the Li-rich member of the series, $La_{0.5}Li_{0.5}TiO_6$.

## Introduction

Interest in lithium conducting solids has increased over the last years because of their potential application in lithium rechargeable batteries.[1,2] In particular, the ionic conductivity of $Li_{3x}La_{\frac{1}{3}-x}TiO_3$ perovskites is one of the highest reported values in lithium crystalline conductors ($10^{-3}$ $\Omega^{-1}$ $cm^{-1}$ at $T = 300$ K).[3–7] The knowledge of the subtle features of their crystal structures is crucial to the understanding of the Li ionic mobility within the La–Ti–O framework. In these perovskites, the tilt of the $TiO_6$ octahedra is a predominant feature that introduces structural distortions affecting Li mobility. The precise structure determination of these oxides by X-ray diffraction is particularly difficult as the superlattice reflections associated with the tilting of the $TiO_6$ octahedra arise from the oxygen atoms, weak scatterers if compared with La and Ti; hence neutron diffraction measurements are more suitable for these investigations.

In recent work, we have used the neutron diffraction technique to determine the tilt of the $TiO_6$ octahedra in the Li-rich member of this series, $La_{0.5}Li_{0.5}TiO_3$, described in the rhombohedral $R\bar{3}c$ space group.[8] Moreover, we have located Li cations at unexpected crystallographic positions, in the center of the square planar windows defined by each four $TiO_6$ octahedra. The large multiplicity of this site favored the huge mobility of $Li^+$ cations in this perovskite, considered among the fastest Li-ion conductors. The situation is still more complex in the Li-poor members of the series: as the lithium content decreases, the amount of vacancies increases, giving rise to a lanthanum/vacancy ordering scheme in alternating planes along the *c*-axis, combined with a particular tilt of the octahedra. An X-ray diffraction (XRD) analysis of the patterns suggested an orthorhombic symmetry for the Li-poor samples.[7,9] However, a precise determination of polyhedra distortion and the octahedral tilting has not yet been undertaken. This determination is particularly justified in this case because previous mobility measurements suggest, unlike the Li-rich member, a bi-dimensional character in dc conductivity.[9]

In this paper, the structure of a Li-poor perovskite, with composition $Li_{0.12}La_{0.63}TiO_3$, has been analyzed by neutron diffraction. We report on the nature of the observed superstructure, accounting for the effect of tilt of $TiO_6$ octahedra and the ordering of La vacancies.

## Results and discussion

The X-ray powder diffraction pattern of $Li_{0.12}La_{0.63}TiO_3$ (inset of Fig. 1) is characteristic of a perovskite structure and displays an excellent crystallinity. This pattern was indexed with an orthorhombic unit-cell of parameters $a \approx 3.863$, $b \approx 3.873$ and $c \approx 7.788$ Å. The doubling of the *c* axis with respect to that of the ideal perovskite structure ($a_o \approx 3.873$ Å) is due to the ordering of the La cations and vacancies in alternating planes along this crystallographic direction. However, this simple description of the unit cell of the perovskite disregards the effect of tilt of the $TiO_6$ octahedra.

The neutron powder diffraction (NPD) pattern of this perovskite displays additional peaks which cannot be indexed with the cell dimensions deduced from the XRD analysis. These superstructure peaks arise from the oxygen shifts inherent to the octahedral tilt, and could be indexed, in a first attempt, in a monoclinic $\sqrt{2}a_o \times \sqrt{2}a_o \times 2a_o$ unit cell, with $a = 5.484$, $b = 5.484$, $c = 7.749$ Å and $\gamma = 90.43°$. We adopted the *P*112/*n* space group, which is a monoclinic subgroup of the orthorhombic *Pban* originally used by MacEachern *et al.*[10] for $La_{0.66}TiO_3$. The Rietveld analysis carried out in *P*112/*n* reproduced most of the NDP features; however, several high-angle peaks were not well fitted, yielding large discrepancy factors ($R_B = 10.7\%$), which suggests that the size of the primitive monoclinic unit cell was not large enough.

We subsequently indexed all the diffraction peaks in a larger unit cell with $2a_o \times 2a_o \times 2a_o$ dimensions, as suggested by Inaguma,[11] and obtained good agreement factors with the pattern matching technique for the unit-cell parameters $a = 7.727$, $b = 7.749$ and $c = 7.786$ Å. Systematic extinctions ($h + k = 2n + 1$) suggested a face-centered *C*-type lattice. Trials to solve the structure in the space groups *Cmmm*, *Cm*2*m* and *Cmm*2, were tested in independent Rietveld analyses, adopting as starting structural model that of the $NH_4MnCl_3$ perovskite (space group: *Cmmm*).[12] This analysis led to the conclusion that the space group that better describes the NDP data is *Cm*2*m* ($R_B = 4.8\%$). Agreement factors obtained with space groups *Cmm*2 ($R_B = 6.7\%$) and *Cmmm* ($R_B = 13.5\%$) were appreciably higher. In this preliminary analysis, $Li^+$ ions were not considered, because of their weak diffraction power (0.12 atoms per formula unit) in the global unit cell. The atomic positions,

 DOI: 10.1039/b109926b

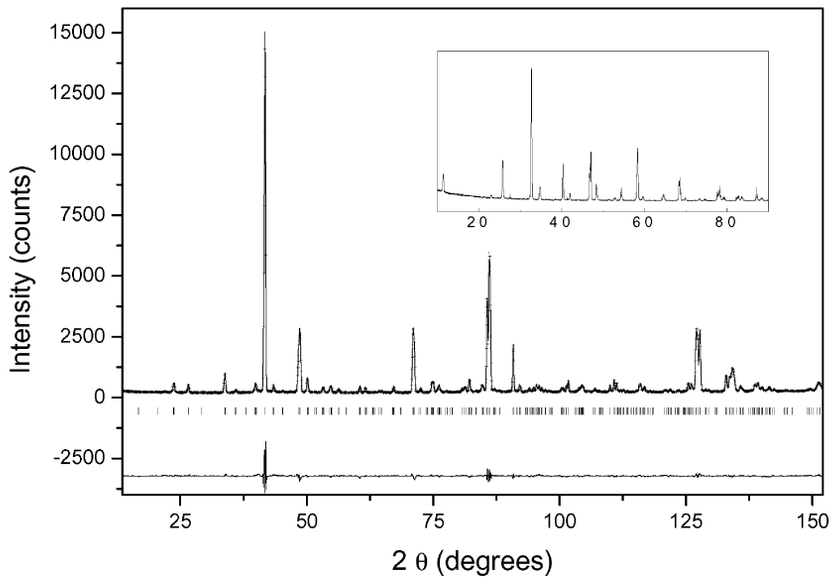


**Fig. 1** Observed (+), calculated (—) and difference (at the bottom) NPD profiles for $Li_{0.12}La_{0.63}TiO_3$ at 295 K. The inset shows the XRD diagram of this sample.

**Table 1** Structural parameters of $Li_{0.12}La_{0.63}TiO_3$ at 295 K [a]

| Atom | *x*/*a* | *y*/*b* | *z*/*c* | $B_{iso}$ | Occupany |
|---|---|---|---|---|---|
| La1 | 0.0000 | 0.0234(4) | 0.0000 | 0.84(6) | 1.01(2) |
| La2 | 0.0000 | 0.0271(4) | 0.5000 | 0.59(5) | 0.29(1) |
| La3 | 0.0000 | 0.5288(5) | 0.0000 | 0.30(4) | 0.88(2) |
| La4 | 0.0000 | 0.5360(4) | 0.5000 | 0.49(4) | 0.30(1) |
| Ti | 0.2493(5) | 0.2662(5) | 0.2605(4) | 0.57(5) | 4.00 |
| O1 | 0.7529(5) | 0.0220(5) | 0.2338(4) | 1.20(10) | 4.00 |
| O2 | 0.0000 | 0.2740(5) | 0.2151(4) | 0.79(10) | 2.00 |
| O3 | 0.0000 | 0.7821(6) | 0.7398(5) | 1.04(11) | 2.00 |
| O4 | 0.7723(5) | 0.7736(5) | 0.0000 | 0.89(10) | 2.00 |
| O5 | 0.2323(5) | 0.2876(5) | 0.5000 | 1.09(10) | 2.00 |

[a] Space group: *Cm*2*m* (38). $a = 7.72605(9)$, $b = 7.74809(8)$, $c = 7.78494(8)$ Å. Agreement factors: $R_B = 4.8\%$, $R_P = 4.0\%$, $R_{WP} = 5.6\%$, $\chi^2 = 4.9$. In this structural refinement Li ions were not included due to their low scattering factor.

occupation of A-sites, and thermal factors are given in Table 1. The quality of the NPD fit is shown in Fig. 1. Thermal factors for La, Ti and O in the NPD analysis are all reasonable (Table 1).

A view of the crystal structure of $Li_{0.12}La_{0.63}TiO_3$ is displayed in Fig. 2, showing that alternating planes along the *c*-axis display different La occupancies. This effect is responsible for the *c*-axis doubling. Additionally, there is an antiphase tilt of the $TiO_6$ octahedra along the *b* (binary) axis, much more important in magnitude than those observed along the *a* and *c* axes. This tilt scheme could be defined as $(0\varphi\psi)$, with $\psi \approx 0$; $\varphi = 6.5°$ ($a^0b^-c^+$ in Glazer's notation).[13] This octahedral tilt pattern is similar to that deduced in this work for the monoclinic *P*112/*n* space group, and that deduced by MacEachern[10] for the $La_{0.66}TiO_3$ perovskite in the *Pban* space group, both with a $\sqrt{2}a_o \times \sqrt{2}a_o \times 2a_o$ unit cell. However, in the case of the $2a_o \times 2a_o \times 2a_o$ superstructure (*Cm*2*m* space group), the direction of the antiphase tilt of the octahedra is perpendicular to the *c*-axis, along which lanthanum and vacancies ordering is produced.

The crystal structure contains four independent sites for La, and only one for Ti. A deeper analysis of the structure shows that the La ions preferentially occupy La1 and La3 crystallographic sites at $z/c = 0$ planes, and the remaining lanthanum and vacancies are accommodated at La2 and La4 sites in $z/c = 0.5$ planes. In this arrangement, averaged ⟨La1–O⟩ and ⟨La3–O⟩ distances (2.68 and 2.70 Å) are considerably shorter than ⟨La2–O⟩ and ⟨La4–O⟩ distances (2.79 and 2.81 Å), the latter corresponding to the vacancy-rich planes. The existence of two

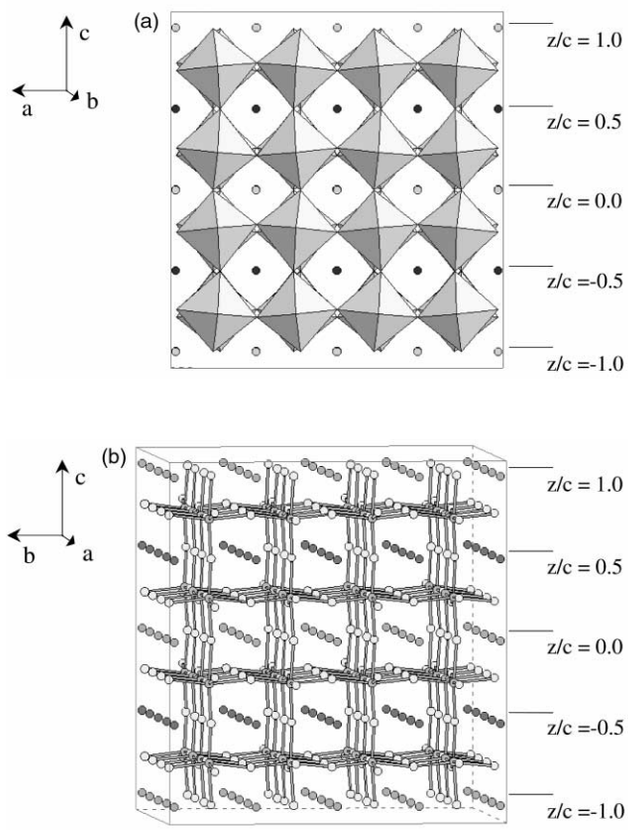


**Fig. 2** Two views of the crystal structure of $Li_{0.12}La_{0.63}TiO_3$, showing: (a) the antiphase tilting of the $TiO_6$ octahedra along the *b* axis, and (b) the absence of tilting along the *a* direction. Differences in La coordination in $z/c = 0$ (fully occupied) and 0.5 (partially occupied) planes are also visualized.

crystallographic sites at $z/c = 0.5$ could favor an alternating disposition of La and vacancies in this plane; however, the very similar occupancy factors found for both sites (0.29 and 0.30, respectively) seems to exclude this possibility.

In this perovskite, the Ti atoms are shifted from the center of the octahedra towards the vacancies-rich plane at $z/c = 0.5$, to compensate for the asymmetric distribution of charges around the octahedra. This fact produces a significant distortion of octahedra, with two significantly different Ti–O distances along the *c*-axis, of 1.88 and 2.04 Å (Table 2). In the *ab* plane, the

**Table 2** Main interatomic distances (Å) and angles (°) in $Li_{0.12}La_{0.63}TiO_3$

| | | | |
|---|---|---|---|
| Ti–O4 | 2.037(1) | Ti–O1′ | 1.993(1) |
| Ti–O5 | 1.876(1) | Ti–O3 | 1.940(1) |
| Ti–O1 | 1.903(1) | Ti–O2 | 1.960(1) |
| ⟨Ti–O⟩ | 1.949(1) | | |
| ⟨O–Ti–O4⟩ | 84.3(1) | ⟨O–Ti–O5⟩ | 95.5(1) |
| ⟨O–Ti–O⟩ | 89.8(1) | ⟨Ti–O–Ti⟩ | 167.8(2) |
| ⟨La1–O⟩ | 2.679(2) | ⟨La3–O⟩ | 2.704(2) |
| ⟨La2–O⟩ | 2.785(2) | ⟨La4–O⟩ | 2.808(2) |
| ⟨Li–O⟩[a] | 1.840 | ⟨Li–O⟩[a] | 2.100 |

[a] Li–O distances deduced from the Fourier map differences (see text).

Ti–O distances are also split into one short (1.90 Å), two medium (1.94, 1.96 Å) and one long (1.99 Å) bond-lengths. The shift off center of Ti could be responsible for the incipient antiferroelectric behaviour described for this compound.[14]

In this family of perovskites, oxygen square windows connecting contiguous A sites act as bottlenecks for Li diffusion. Our NPD data show that diagonal O–O distances are appreciably bigger in square windows that connect A sites along the *a* axis (3.88–4.15 Å), suggesting that the mobility of Li could be favored along this axis with respect to the two other directions (3.59–4.43 Å for *b*; 3.82–3.95 Å for *c*-axis). Taking into account that the amount of cation vacancies is considerably higher in planes-*ab* with $z/c = 0.5$ than in planes with $z/c = 0$, it is reasonable to assume that Li mobility should be enhanced in alternating *ab* planes with $z/c = 0.5$, and within these planes preferentially along the *a*-axis. Along the *b*-axis the alternating rotation of contiguous octahedra reduces the cross section for Li diffusion (see Fig. 2). These structural features are in good agreement with the low dimensionality of Li mobility, measured at low temperatures in these materials.[9]

As a final stage of this analysis, possible positions for $Li^+$ cations were investigated. A Fourier synthesis performed over the difference between observed and calculated structure factors deduced by Rietveld refinement (including La, Ti and O positions), yields information on the location of the "missing" atoms.[8] In this analysis, the negative scattering length of Li favors its location. A difference Fourier map showed a weak negative peak at (0,0.31,0.5), in the plane $z/c = 0.5$ where La vacancies are accumulated. This position is very close to that reported for $Li^+$ ions in the rhombohedral $La_{0.5}Li_{0.5}TiO_6$ perovskite. Nevertheless, the incorporation of Li atoms at these positions, with the appropriate stoichiometry, 0.12 per formula unit, did not significantly improved the $R_B$ factor in a non-constrained refinement, as a consequence of the weak scattering power of lithium in this perovskite. In order to confirm this point this analysis should be extended to other orthorhombic samples with higher Li contents.

As a final remark, it must be noted that the octahedral tilting scheme observed in $Li_{0.12}La_{0.63}TiO_3$ along the *b*-axis, described in a simplified way as $(0\ \varphi\ 0)$, differs from that reported for the Li-rich member, $Li_{0.5}La_{0.5}TiO_3$, along the three axes $(\varphi\varphi\varphi)$ ($a^-a^-a^-$ in the Glazer's notation).[8] Other important differences between both perovskites is the distribution of La vacancies. Both facts are closely connected with the three-dimensional mobility reported for lithium in the latter case, in contrast to the lower dimensionality detected in the perovskite analysed in this work.

## Conclusions

The NPD structural analysis carried out in the Li-poor member ($x = 0.04$) of the $Li_{3x}La_{\frac{2}{3}-x}TiO_3$ series, allowed us to determine the ordered distribution of La and vacancies over alternating *c*-planes of the perovskite. The vacancies distribution accounts for the significant distortion in Ti oxygen coordination, producing the off center shift of the $Ti^{4+}$ cations. In the superstructure $2a_0 \times 2a_0 \times 2a_0$ adopted by this phase, octahedral $TiO_6$ tilting is responsible for the axis doubling detected. Both structural features, namely the octahedral tilt and alternating cation vacancies distribution, are responsible for the bi-dimensional mobility of $Li^+$-ions reported at low temperatures. The 2-D lithium mobility in Li-poor members, contrasts with the three-dimensional character of lithium conductivity in the Li-rich member of the series, $Li_{0.5}La_{0.5}TiO_3$.

## Experimental

The $Li_{0.12}La_{0.63}TiO_3$ sample was prepared in polycrystalline form by heating at 1150 °C a stoichiometric mixture of high purity and previously dried $Li_2CO_3$, $La_2O_3$ and $TiO_2$ reagents. The reacted powder was made into a pellet and fired at 1350 °C in air for 6 h. The metal molar ratio was confirmed by inductively coupled plasma spectroscopy (ICP) using a JY-70 plus spectrometer. In order to reduce the absorption cross section in the neutron experiments, $^7Li$ enriched samples were prepared. X-Ray diffraction patterns were collected with Cu-Kα radiation indicating the absence of any impurity. The neutron powder diffraction (NPD) pattern was collected at the high resolution D2B diffractometer at ILL-Grenoble. A wavelength of 1.594 Å was selected from a Ge monochromator. The counting time was 4 h, using about 4 g of sample contained in a vanadium can. The FULLPROF program[15] was used to perform the profile refinement. A pseudo-Voigt function was chosen to reproduce the line shape of diffraction peaks. In this analysis, the coherent lengths for La, Li, Ti and O were 8.24, −1.90, −3.438 and 5.803 fm.


## Acknowledgements

The authors thank C. León and J. Santamaría for helpful discussions and ILL for provision of neutron beam time. We also thank the Spanish CICYT (MAT2001–0539, MAT98–1053–C04–03 and MAT2001–3713–C04–03 projects) for financial support.


## References


1 K. M. Colbow, J. R. Dahn and R. R. Haering, *J. Power Sources*, 1989, **26**, 397.
2 A. D. Robertson, A. R. West and A. G. Ritchie, *Solid State Ionics*, 1997, **104**, 1.
3 A. G. Belous, G. N. Novitskaya, S. V. Polyanetskaya and Y. I. Gornikov, *Zh. Neorg. Khim.*, 1987, **32**, 283.
4 Y. Inaguma, L. Chen, M. Itoh, T. Nakamura, T. Uchida, H. Ikuta and M. Wakihara, *Solid State Commun.*, 1993, **86**, 689.
5 H. Kawai and J. Kuwano, *J. Electrochem. Soc.*, 1994, **141**, L78.
6 O. Bohnke, C. Bohnke and J. L. Fourquet, *Solid State Ionics*, 1996, **91**, 21.
7 J. Ibarra, A. Várez, C. León, J. Santamaría, L. M. Torres-Martinez and J. Sanz, *Solid State Ionics*, 2000, **134**, 219.
8 J. A. Alonso, J. Sanz, J. Santamaría, C. León, A. Várez and M. T. Fernandez-Diaz, *Angew. Chem., Int. Ed*, 2000, **3**, 619.
9 M. A. Paris, J. Sanz, C. Leon, J. Santamaría, J. Ibarra and A. Varez, *Chem. Mater.*, 2000, **12**, 1694.
10 M. J. MacEachern, H. Dabkowska, J. D. Garrett, G. Amow, W. Gong, G. Liu and J. E. Greedan, *Chem. Mater.*, 1994, **6**, 2092.
11 Y. Inaguma, T. Katsumata and M. Itoh, *Proceedings of the International Workshop on LLTO*, Le Mans, 2001, 4.
12 J. Tornero, F. H. Cano, J. Fayos and M. Martinez-Ripoll, *Ferroelectrics*, 1978, **19**, 123.
13 A. M. Glazer, *Acta Crystallogr., Sect. B*, 1972, **28**, 3384.
14 M. L. Sanjuán and M. A. Laguna, *Phys. Rev. B*, 2001, **64**, 174305.
15 J. Rodriguez-Carvajal, *Physica B*, 1992, **192**, 55.